BRILL
WAGENINGEN
ACADEMIC

JOURNAL OF INSECTS AS FOOD AND FEED (2025) DOI:10.1163/23524588-BJA10334

Journal of Insects as Food and Feed
brill.com/jiff

RESEARCH ARTICLE

Colourimetric characterization of naturally-coloured cocoons in a silkworm germplasm collection

Gianni Fila[1]*, *Massimo Gardiman*[2], *Alessio Saviane*[1], *Chiara Pavanello*[1] *and Silvia Cappellozza*[1]

[1]Research Centre for Agriculture and Environment (CREA-AA), Sericulture Laboratory, Council for Agricultural Research and Economics, Via Leonardo Eulero 6a, 35143 Padova, Italy; [2]Research Centre for Viticulture and Enology (CREA-VE), Council for Agricultural Research and Economics, Via XXVIII Aprile 26, 31015 Conegliano (TV), Italy; *gianni.fila@crea.gov.it

Received 12 September 2025 | Accepted 7 November 2025 | Published online 25 November 2025

Abstract

Cocoon colour in *Bombyx mori* L. is a genetically determined trait influenced by environmental factors, reflecting the natural pigments embedded in silk proteins, which may have potential applications in the feed and food industry. We quantified cocoon colour across 65 naturally coloured strains belonging to the silkworm germplasm collection of CREA, which were reared over three seasons, and assessed practical systems for colour classification. Colours were measured in CIELAB (D65/10°; SCI/SCE recorded simultaneously), and colour-difference models were benchmarked against human perception via an observer-based grouping task analysed with non-metric MDS. CIEDE2000 model best matched perceptual distances. Two perceptibility thresholds were derived: ΔE_{50} = 3.65 (noticeable to 50% of observers) and ΔE_{100} = 7.2 (universally noticeable). Intra-strain variability generally remained below ΔE_{100}, whereas interannual variability exceeded it in roughly one-third of strains. At the strain level, chromatic change in the a^*b^* plane was predominantly linear, with either radial (chroma-driven) or non-radial (hue-shifting) behaviour. At the collection level, colours formed discrete clusters; using ΔE^*-constrained clustering yielded 7 clusters. Among nomenclature systems, RHS (Royal Horticultural Society colour chart) offered the highest resolution but required many codes per strain; UCL (Universal Colour Language, based on RHS) provided broader but more consistent categories covering the observed gamut with approx. 3 codes per strain. We recommend a standardised, ΔE^*-anchored, cluster-based scheme for sericulture applications; when external references are preferred, a compact UCL-RHS combination reliably characterises strain colour while remaining practical.

Keywords

cocoon – colour – colorimetric measurements – CIEDE2000 – silkworm

1 Introduction

The silkworm (*Bombyx mori* L.) produces cocoons of various colours, including white, yellow, golden yellow, pinkish, orange and green, which derive from the pigments found in mulberry leaves which the insect feeds on. The pigments found in leaves are first absorbed by the midgut and then conveyed into the haemolymph. Subsequently, they enter the silk glands, where they accumulate and are enclosed in the silk proteins' layers to finally produce colourful cocoons. Chemical modifi-

cations of the pigments can occur during the stages of this process (Tabunoki *et al.*, 2004).

There are essentially two varieties of cocoon colours: those derived from carotenoids (Ma *et al.*, 2015), which are responsible for the yellow-orange colours and are found only in sericin which coats the fibroin base, and those derived from flavonoids (mainly quercetin and kaempferol and their glycosides) (Kurioka and Yamazaki, 2002; Zhu and Zhang, 2014), which are responsible for the green hues and are distributed in both sericin and fibroin. Cocoon colour has long been recognized as a genetically determined trait (Tanaka, 1913), yet the molecular mechanisms underlying this genetic determinism have only recently begun to be elucidated (Daimon *et al.*, 2010; Hirayama *et al.*, 2018; Lu *et al.*, 2023; Tsuchida and Sakudoh, 2015; Zhu and Zhang, 2014).

From an evolutionary perspective, variability in cocoon colour may represent a selective adaptation linked to protective functions. The pigments responsible for colouration possess antibacterial and antioxidant properties, contributing to larval defence against pathogens and oxidative stress during pupation (Dong *et al.*, 2022; Liu *et al.*, 2024). Beyond their ecological role, these pigments are increasingly studied as bioactive compounds with potential practical applications in medicine, nutraceuticals, and cosmetics. This emerging field aligns with the broader concept of entomoceuticals, which refers to health-promoting compounds derived from insects, including proteins, polyphenols, terpenoids, alkaloids, and carotenoids, many of which exhibit anti-inflammatory, antioxidant, antihypertensive, and antidiabetic properties (Liceaga, 2025).

In the case of *Bombyx mori*, cocoon pigments are primarily associated with sericin, a protein that not only provides structural stability but also carries bioactive molecules and trace elements with therapeutic potential (Biganeh *et al.*, 2022; Wang *et al.*, 2025). Coloured sericin enriched with carotenoids, has been shown to outperform white cocoon sericin in antibacterial, antioxidant, cytocompatibility, and even anticancer activities, due to structural modifications such as increased β-sheet content and hydrogen bonding, which enhance its stability and functional properties (Liu *et al.* 2024).

Among the carotenoids found in yellow-red cocoons, lutein occurs in a protein-lipid bound form, which is chemically stable and exhibits superior antioxidant activity compared to purified commercial lutein (Manupa *et al.*, 2023). Its bioavailability and stability make it a promising dietary supplement for ocular and cognitive health, with demonstrated protective effects against UV-induced retinal damage (Aimjongjun *et al.*, 2013) and β-amyloid-induced neurotoxicity in neuronal cells, thus suggesting potential in the prevention of age-related macular degeneration and Alzheimer's disease (Singhrang *et al.*, 2018). In addition, lutein extracts from silk cocoons have shown immunomodulatory effects, enhancing both innate and adaptive immunity beyond what has been observed with marigold-derived lutein (Promphet *et al.*, 2014). The hypoglycaemic potential of sericin-derived oligopeptides (SDOs) from yellow cocoons has been validated in diabetic rat models, where they improved glycaemic control, preserved pancreatic function, and protected multiple organs from diabetes-related damage (Tocharus and Sutheerawattananonda, 2024).

Flavonoid-rich ethanol extracts from green cocoons exhibit strong antioxidant activity together with tyrosinase and α-glucosidase inhibition, whereas highly purified sericin alone shows limited bioactivity (Cao and Zhang, 2016; Wang *et al.*, 2012). These extracts have also been shown to improve glucose metabolism, enhance antioxidant defences, and increase insulin sensitivity in diabetic models, supporting their use in the prevention or management of type 2 diabetes (Tian *et al.*, 2024; Wang *et al.*, 2020; Zhao *et al.*, 2019). Furthermore, flavonoid-sericin conjugates display enhanced antioxidant and anti-inflammatory activities compared with native sericin, expanding their biomedical potential (Omar *et al.*, 2022). Beyond therapeutic applications, coloured cocoon sericin has also been suggested as a natural antioxidant ingredient in functional foods (Takechi *et al.*, 2011). Among the features connected with the green colour is the capacity to protect skin after radiation (Kakihara *et al.*, 2024).

Overall, the bioactivities attributed to cocoon pigments provide strong evidence for their inclusion in functional foods, nutraceuticals, and biomedical applications. Variability in cocoon pigmentation, once considered mainly as an adaptive trait for insect survival, thus emerges as a key reservoir of health-promoting compounds with translational potential for human applications.

Research on natural cocoon colours is particularly relevant also to silk textiles, offering the possibility of producing environmentally sustainable yarns without reliance on synthetic dyes which are a significant cause of pollution (Moore and Ausley, 2004; Robinson *et al.*, 2001).

Furthermore, it should be noted that there is the possibility of producing non-textile silk-based products

(Oxman, 2015; Oxman *et al.*, 2013) which, not being subjected to the degumming process, can retain their natural colour.

The renewed interest in cocoon pigmentation underscores the need for precise, standardized colour descriptors in silkworm strain characterization. While pigment chemistry is well studied, quantitative colour analysis has lagged, partly due to environmental influences on this continuous trait. Investigating cocoon colour offers several advantages over biochemical analyses. Instrumental colour measurement is rapid, non-destructive, and scalable; moreover, in many plant-based systems, CIELAB coordinates correlate with underlying pigment content, enabling colour to serve as an informative proxy (Afonso *et al.*, 2017; Ayour *et al.*, 2016; Chen *et al.*, 2023; Conesa *et al.*, 2019; Lancaster *et al.*, 1997; Lu *et al.*, 2021; Singha *et al.*, 1991), and this may also apply to cocoons, whose pigments are entirely plant-derived.

In this study we examine cocoon colorimetric variability across a wide collection of silkworm strains and evaluate whether each strain can be reliably associated with a defined colour or set of colours. We also seek a practical, robust classification framework suitable for strain identification, conservation, and valorisation of sericultural genetic resources.

2 Materials and methods

Silkworm rearing and cocoons preparation

The Sericulture Laboratory of CREA-AA in Padua maintains 177 silkworm strains, constituting the largest germplasm collection currently maintained in Europe. In this collection, 65 strains with naturally coloured cocoons have been studied; they are listed in Table S1 of the Supplementary Materials. Insects are reared under standard conditions on fresh mulberry leaves, harvested daily or stored up to 72 h at 12 °C in the dark. To preserve genetic diversity and limit inbreeding, 400 cocoons are collected annually from each strain. At least 72 mating pairs are set up, producing an equal number of egg batches, which are split into two replicates. One replicate is used to rear the next generation (2.5 g of eggs brushed), while the other is stored as reserve.

Cocoons were de-flossed, cut to extract pupae (preventing moth urine from staining fibres), and stored at 5 °C in the dark until colorimetric measurements, performed within three weeks of spinning.

Most strains were reared in April-May, when mulberry leaves are most abundant, with some reared in September-October to balance workload. The same strains were reared in the same season across the three-year study.

Instrumental colour measurements

Colour assessments were conducted over three consecutive years (2022-2024), with ten cocoons per strain measured in 2022 and 2023, and twenty in 2024. Measurements were performed in the CIE 1976 $L^*a^*b^*$ colour space (CIE, 2019) using a spectrophotometer (CM-2500d, Konica Minolta Sensing, Japan). The L^* parameter indicates lightness, ranging from 0 (black) to 100 (white), a^* represents the green-red axis, with negative values corresponding to green and positive values to red, and b^* represents the blue-yellow axis, with negative values indicating blue and positive values yellow.

Measurements were taken on the external surface of each cocoon. A standard 8-mm-diameter measurement aperture was used to define the sample area, with settings configured for a D65 standard illuminant and a 10° standard observer. Measurements were carried out in both specular components included (SCI) and specular component excluded (SCE) modes.

Choosing the best equation for colour difference measurement

Data processing involved calculating colour distance (ΔE^*) to assess the degree of similarity or dissimilarity between two colours. The simplest known formula to compute ΔE^* is given by the Euclidean distance, which is the CIE76 method (Robertson, 1977), but since the CIELAB colour space is not perceptually uniform as equal Euclidean distances do not always correspond to equal perceptual differences, many alternative formulas exist to address this limitation (Luo, 2002). Each of these has been optimised for specific datasets, varying in scale, material type, colour differences, and sample dimensions, which may limit their applicability to other contexts. As no prior studies have evaluated models for characterising colour differences in silkworm cocoons, we conducted an experimental comparison of the most advanced colour difference formulae, i.e. CIE76, CMC (Clarke *et al.*, 1984; McDonald, 1988), CIE94 (McDonald and Smith, 1995; Melgosa, 2016) and CIEDE2000 (Luo *et al.*, 2001; Sharma *et al.*, 2005). The CIEDE2000 colour difference equation is the latest evolution of the CIE76 and it is the one most used in textile industry (Luo *et al.*, 2001).

The formulae were tested following Gomez-Polo *et al.* (2016). Twenty participants (8 males, 12 females; 18-60 years) individually sorted 40 cocoons, selected to cover the full colour range of the collection, into perceptual

groups of their choice under standard illumination on a neutral grey background. For each participant, results were encoded in a 40 × 40 binary matrix (1 = same group; 0 = different groups). Matrices were summed to obtain an aggregate similarity matrix *S*, from which a dissimilarity matrix *D* was derived as $D = N\_observers - S$. Matrix *D* was symmetric, ranging from 0 (all grouped together) to 20 (none grouped together).

Non-metric Multidimensional Scaling (MDS; Kruskal, 1964) was applied to *D* using the MASS package in R (v. 7.3-65; R Core Team, 2022; Ripley *et al.*, 2023; Venables and Ripley, 2002). Model fit was assessed with stress (S-stress) and R^2. Pairwise Euclidean distances from the MDS configuration were then correlated (Pearson's *r*) with ΔE^* values calculated using alternative colour difference formulas. The formula showing the highest correlation was deemed most consistent with human perception and was subsequently used for further processing, including the establishment of an acceptability threshold for colour difference. The procedure is described in full detail in Annex S2 of the Supplementary Materials.

Pattern detection in $L^*a^*b^*$ variability: PCA and cluster analysis

The analysis aimed to identify systematic patterns in colour distribution within and across strains. In the first part of the analysis, a^* and b^* coordinates were examined for each strain using PCA (centred, unscaled) to capture the two-dimensional variance structure. From PCA we extracted eigenvalues (λ_1, λ_2), linearity ratio (λ_1/λ_2), variance explained by PC1, eccentricity (σ_1/σ_2), and the slope/intercept of the first principal axis. In parallel, linear regression ($b^* \sim a^*$) was performed to obtain slope, intercept, R^2, and intercept significance. These metrics described the geometry, orientation, and coherence of chromatic distributions, enabling comparison of structural patterns across strains.

In the second phase of the analysis, the DBSCAN algorithm (Ester *et al.*, 1996) was applied to identify clusters representing regions where colours exhibited a natural tendency to aggregate. DBSCAN detects dense point regions based on distance (ε) and minimum points (*minPts*). As point density varied across colour space, the dataset was partitioned into regions of similar density, and the algorithm was applied separately to each.

Intra- and inter-annual within-strain variability

Intra- and inter-annual chromatic variability was analysed to assess the stability of cocoon colour. Intra-annual variability was quantified by calculating all pairwise ΔE^* values within each strain and year, generating distributions to be compared against ΔE_{50} and ΔE_{100}. Inter-annual variability was assessed by computing pairwise ΔE^* values across all year-to-year strain combinations.

Evaluation of colour classification systems

Instrumental systems such as CIELAB provide precise values but are not intuitive for practical use. Standard references like Pantone® or RAL enable accessible visual classification, differing in resolution: finer categories allow greater discrimination, while broader ones offer tolerance and simplicity. For applied purposes, widely recognised systems are preferable, ideally offering broad coverage, few categories, low within-group variability, and clear separation.

We compared clustering of our dataset (CA – cluster analysis) with the Royal Horticultural Society (RHS) Colour Chart and two derived schemes: RHS-UPOV (UPOV hereafter) and RHS-UCL (UCL hereafter), shortly described below.

RHS colour chart: The RHS Colour Chart (Royal Horticultural Society, 1966) provides a standardised reference for plant variety description and was deemed suitable for cocoon colours, which derive from plant pigments. In this study, RHS codes were assigned to observations using the 2007 edition (892 swatches) and the ColourNameR package (Sánchez Beeckman, 2022) for $L^*a^*b^*$-to-RHS conversion.

UPOV nomenclature: Because the RHS chart is overly detailed for plant variety description, UPOV (International Union for the Protection of New Varieties of Plants, https://www.upov.int) developed a simplified system grouping RHS colours into 73 broad categories (e.g. Pink, Medium Red, Dark Purple), each with standardised names in four languages. UPOV names used here were retrieved with the ColourNameR package.

UCL nomenclature: The Universal Colour Language (UCL), developed by the Inter-Society Color Council-National Bureau of Standards (ISCC-NBS), was used in 1984 by the American Rhododendron Society (ARS) to classify RHS codes (1966 edition) (Huse and Kelly, 1984). These assignments were later revised based on spectrophotometric measurements (Voss, 2002; Voss and Hale, 1998). For the purposes of this study, UCL names corresponding to RHS codes were obtained from the official website of the Office of the American Rhododendron Society (Office of the American Rhododendron Society, 2025).

TABLE 1 Pearson's r correlation coefficients between ΔE^* values and MDS distances of the visually assessed similarity matrix for cocoon pairs

Formula	r for ΔE^* ~ MDS intervals
CIE76	0.68***
CMC	0.77***
CIE94	0.80***
CIEDE2000	0.81***

*** $p < 0.001$.

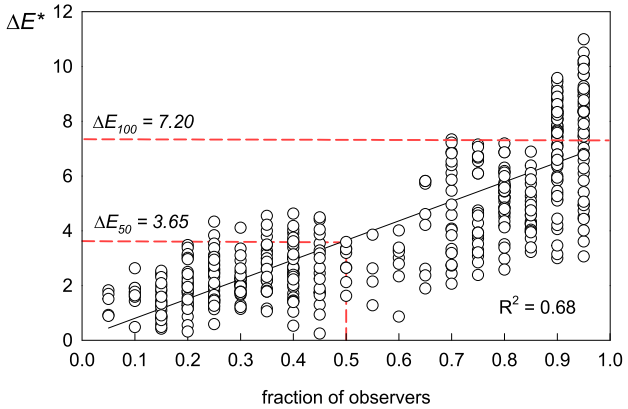

FIGURE 1 Acceptability threshold assessment for cocoon colour differences. x-axis, proportion of observers detecting a difference; y-axis, ΔE^* (CIEDE2000). Each point is one cocoon pair.

3 Results

Instrumental measurement results

Mean values of the CIELAB parameters L^*, a^* and b^* for each strain are reported in Table S1 of Supplementary Materials. The table also includes chromatic classifications based on four reference systems: RHS, UCL, UPOV and CA. Some strains were measured in only one or two years due to health-related issues that prevented the production of regular, classifiable cocoons. For all three parameters, the differences between SCI and SCE remained within ±1% (Figure S1, Supplementary Materials); therefore, all subsequent analyses were carried out using data collected in SCI mode only.

Evaluation of colour distance formulae

The ranges of colour distances observed in the 40 cocoon samples were as follows: CIE76 (0.52-51.00), CMC (0.27-24.61), CIE94 (0.21-20.00) and CIEDE2000 (0.24-14.71) (not shown). Following this, an MDS analysis was conducted on the perceptual similarity matrix, resulting in a two-dimensional coordinate configuration with a final stress value of 0.084, indicating a good fit.

Pairwise Euclidean distances between all cocoon pairs were then computed using the MDS-derived coordinates. These perceptual distances were plotted against the corresponding values from each colour difference formula, and Pearson correlation coefficients (r) were calculated to evaluate the strength of association, as well as their corresponding p-values. The resulting r values are summarised in Table 1.

CIE76 showed the weakest correlation with perceptual distances obtained from visual assessment, whereas CIEDE2000 achieved the strongest correlation, albeit only marginally outperforming CIE94.

Establishing an acceptability threshold value for colour difference

Processed data from the MDS procedure were used to establish reference ΔE^* values. All colour pairs from the visual similarity matrix and their corresponding CIEDE2000 distances were plotted against the proportion of observers who placed each pair in different groups (Figure 1). Data points corresponding to 100% observer agreement were excluded from the regression analysis, as these values deviated from linearity. A linear regression was then fitted to the remaining points. The ΔE^* value corresponding to 50% observer agreement on the fitted line is 3.65, and was identified as the ΔE_{50} acceptability threshold. By extrapolating the line to 100% observer agreement, a ΔE^* value of 7.2 was obtained, representing the ΔE_{100} threshold. The ΔE_{50} threshold may be interpreted as a low-tolerance threshold, while the ΔE_{100} threshold defines a looser boundary. The appropriate threshold to apply depends on the intended use and sensitivity requirements of the analysis.

Overall variability in the $L^*a^*b^*$ colour space

The relative frequency distributions of the CIELAB parameters (Figure 2) reveal patterns of colour variability across the silkworm cocoon dataset. The L^* values exhibit a unimodal distribution, slightly skewed toward higher values, with a dominant peak around $L^* = 82$. The limited spread ($\sigma \approx 4.3$) indicates low variation in lightness. The a^* values display a trimodal distribution, with a main peak near $a^* = 10$ (slightly reddish), a secondary peak in the negative range (greenish tones), and a weaker but still discernible third peak at higher positive values (more saturated reds). The relatively high

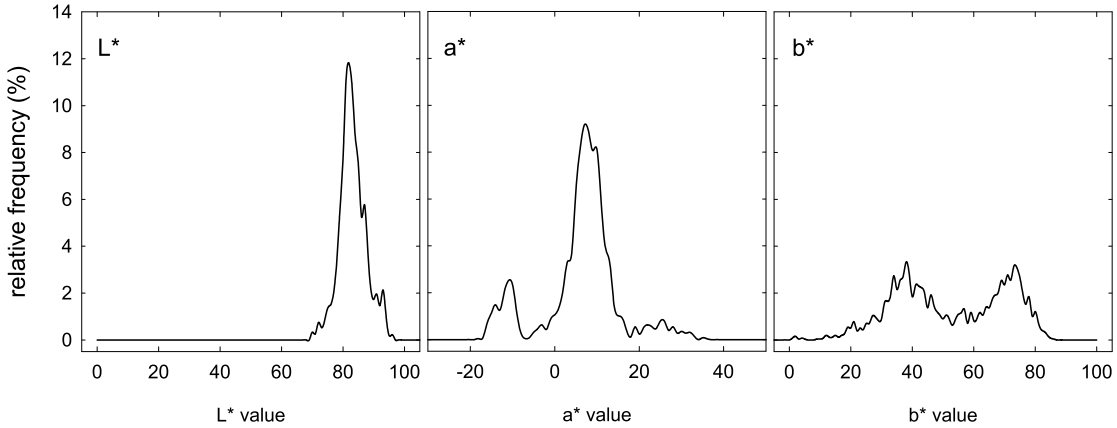

FIGURE 2 Relative frequency distributions (%) of CIELAB colour coordinates (L^*, a^*, b^*) measured on all silkworm cocoons used in this study.

TABLE 2 Summary PCA statistics of chromatic distribution indicators within strains

Indicator	Mean	Median	Min	Max
λ_1/λ_2 (eigenvalue ratio)	26.25	14.46	2.02	365.59
Variance explained by PC1 (%)	91.85	93.53	66.92	99.73
Eccentricity (σ_1/σ_2)	4.39	3.8	1.42	19.12
R^2 (linear regression)	0.5	0.51	0.002	0.94

standard deviation ($\sigma \approx 9.13$) reflects substantial chromatic variability along this axis. The b^* values show a bimodal distribution, with peaks around 40 and approx. 75, reflecting marked variation in the yellow component of cocoon colour. Overall, these patterns highlight limited variation in lightness but pronounced differences along the chromatic axes, particularly a^* and b^*.

Strain-level analysis of chromatic variation patterns

PCA and regression analyses revealed strong linearity in cocoon chromatic data within the a^*b^* plane (Table 2). Eigenvalue ratios (λ_1/λ_2; mean = 26.2, median = 14.5) and variance explained by PC1 (>91%, up to 99.7%) indicated highly anisotropic, with a well-defined dominant direction, near-unidimensional distributions, further supported by eccentricity ($\sigma_1/\sigma_2 \approx 4.4$, max > 19). Slopes from PCA and regression were consistent, with mean $R^2 = 0.50$ (max > 0.93). Thus, chromatic variation is largely linear and directional, likely reflecting pigment gradients or other biological constraints.

From these results it is clear that most strains exhibited a linear pattern of chromatic variation in the a^*b^* plane. Two directional patterns exhibited by the regression line are distinguishable. When the line crosses the origin (radial behaviour), the hue remains approximately constant, and variation occurs primarily in chroma. In contrast, when the line does not intersect the origin (non-radial behaviour), both hue and chroma vary jointly. Applying an empirical criterion (radial: PCA linearity > 5 and |intercept| < 30; non-radial: |intercept| > 40), 30 strains were classified as radial and 26 as non-radial, while the remaining strains displayed intermediate patterns and could not be clearly categorised.

Figure 3 shows examples of strains exhibiting radial behaviour (Fig. 3A), as well as others displaying non-radial or intermediate patterns (Fig. 3B).

Figure S2 in the Supplementary Materials exemplifies the interannual trend of variation in the a^*b^* chromatic space, indicating a directional shift in colour over time across all three example strains. This suggests a consistent temporal change in colour characteristics, independent of strain identity.

Cluster analysis

A preliminary visual inspection of the distribution of the measurements, based on the projection of points onto the a^*b^* plane, revealed that most values were concentrated in the central region of the a^* axis, specifically within the range $0 < a^* < 17$. Measurements falling to the left and right of this interval exhibited lower densities. Accordingly, the algorithm was run separately on three subsets based on a^* values: $a^* < 0$, $0 < a^* < 17$, and $a^* > 17$. Based on the thresholds previously established (Figure 1), the parameter ε, defined as the maximum distance at which two points are perceived as similar, was set to ΔE_{50} for all three subsets. While the *minPts*

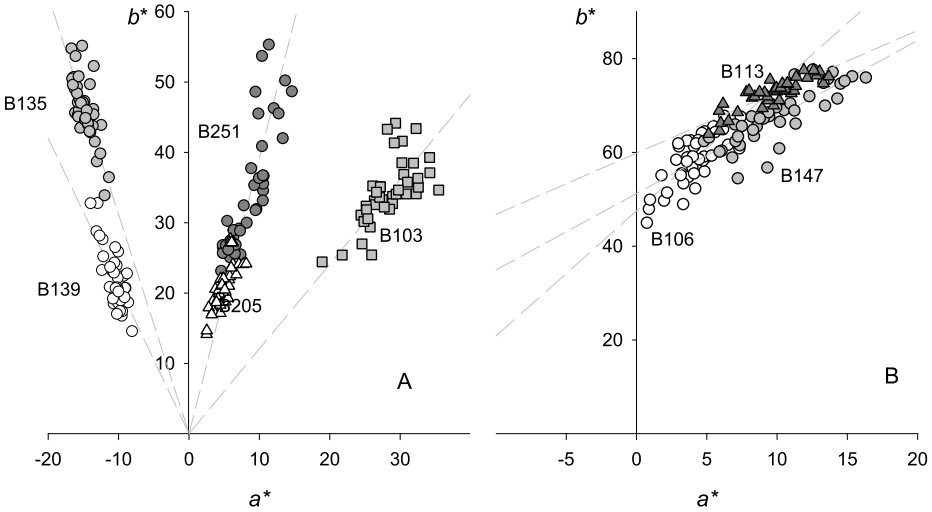

FIGURE 3 Within-strain colour variation patterns in CIELAB space. Symbols represent different genotypes or groups.

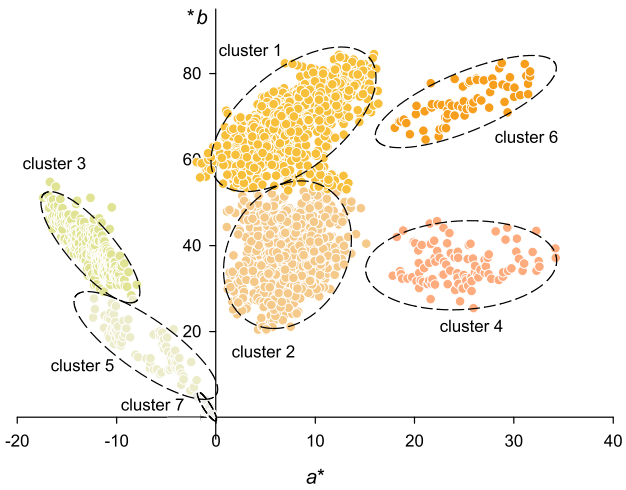

FIGURE 4 Cluster analysis of colour performed using the DBSCAN algorithm. In each cluster, the colour of the symbols corresponds to that of the respective medoids and has been rendered after conversion to sRGB.

parameter, indicating the minimum number of points required to identify a core point, was adjusted to 5 for the two lateral intervals and to 40 for the central interval. These values were determined through a trial-and-error procedure aimed at minimising noise.

The procedure identified seven clusters, as shown in Figure 4. Each cluster has been assigned the colour of its respective medoid. The colours are rendered after conversion to the sRGB system to provide an approximate visual representation of the chromatic tone. Points classified as "noise" (n = 213) are not shown.

Table 3 provides a summary of the characteristics of the identified clusters, with the colour specifications for their medoids, which are the points with the minimum average distance to all other points within the cluster.

To better visualise clusters, they have been enclosed by a 95% confidence ellipse, derived from the covariance matrix of a^* and b^*. Ellipse shape and orientation were determined by eigen decomposition, providing a compact representation of cluster variability and spatial extent in CIELAB space.

Overall colour variability described with classification systems

After classification with RHS, UPOV, UCL and CA, notable differences emerged in the number and distribution of categories. The RHS system yielded 106 colours, with 63 covering 95% of observations; the most frequent was "15A" (19.3%). UPOV grouped colours into 19 categories, with 11 covering 95%; "medium yellow orange" was most frequent (34.1%). UCL produced 27 categories, 15 covering 95%, with "vivid yellow" most common (25.4%); one group (2.4%) had "no name" due to missing labels for RHS codes introduced in 2007 (e.g. N144D, N163D, N163C, N25D, N25C). CA produced only 7 classes, but with highly unbalanced representation: one class held 47% of observations, and two classes together explained over half of the variability. Table 4 summarises these results.

Within-strain variability across intra- and inter-annual scales

Figure 5 offers a concise summary of pairwise distance distributions across all strains, presenting the medians and 95th percentiles for each, benchmarked against two reference red lines corresponding to ΔE_{50} and ΔE_{100}.

As for intra-annual variability, all medians fall below the ΔE_{50} threshold. The 95th percentile remains mostly below ΔE_{100}, with the exception of five strains, which do

TABLE 3 CIELAB of the cluster medoids shown in Fig. 4 and relative colour classification (RHS, UPOV and UCL systems)

Cluster ID	L^*	a^*	b^*	RHS	UPOV group-name	UCL group-name	Cluster size
1	80.51	8.23	70.23	15A	18 (dark yellow)	82 (vivid yellow)	1054
2	83.43	7.31	37.82	22C	20 (medium yellow orange)	70 (light orangish yellow)	789
3	88.51	–12.59	38.31	1C	5 (light yellow green)	101 (light greenish yellow)	285
4	77.09	26.1	35.23	29B	22 (light orange)	52 (light orange)	101
5	92.62	–5.3	16.14	150D	16 (light yellow)	119 (light yellowish green)	84
6	72.42	24.39	72.5	N163D	21 (dark yellow orange)	No name	66
7	93.07	–0.69	1.87	192D	7 (light grey green)	153 (greenish white)	13

TABLE 4 Relative frequency (%) of colours accounting for 95% of the dataset observations, classified according to three nomenclature systems: RHS, UPOV, UCL and CA (cluster analysis)

Colour classification system	Classes accounting for 50% colour variability	Classes accounting for 95% colour variability	Classes accounting for 100% colour variability	Frequency of the most represented class
RHS	12	62	106	19.30%
UPOV	2	11	19	34.10%
UCL	4	15	27	25.4
CA	2	5	7	47.03

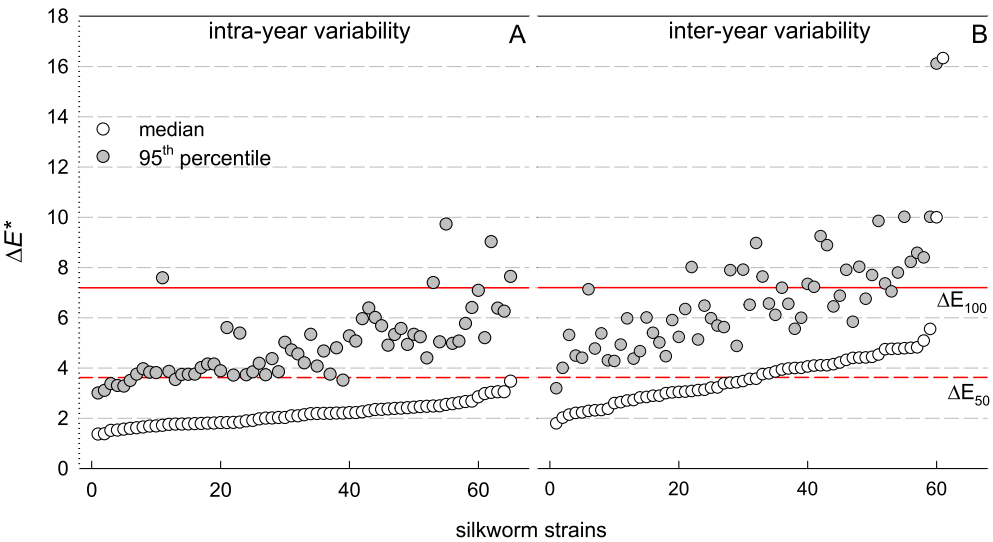

FIGURE 5 Pairwise within-strain ΔE^* distributions summarized by medians (open symbols) and 95th percentiles (grey symbols). Results are shown for within-year comparisons (A) and across-year comparisons (B). Strains are arranged in order of increasing median.

not exceed the ΔE^* value of 10. For six strains, the 95th percentile is even lower than ΔE_{50}.

Inter-annual variability is notably higher. Approximately half of the medians exceed ΔE_{50}, although all remain below ΔE_{100}, apart from a single strain (B102). The 95th percentile exceeds ΔE_{50} in almost all cases and surpasses ΔE_{100} in 18 strains. Notably, for the strain B102, the 95th percentile reaches a maximum value of 16.1.

The ratio between the mean inter-annual distances and the mean intra-annual distance ranged from 0.98 to 2.02 for nearly all strains. Only strains B251 and B102 showed higher ratios of 2.87 and 3.10, respectively (not shown).

Descriptive efficiency of strain colour classification

RHS was the system that required the highest number of classes to describe within-strain variability, with an average of 6.2 labels needed to characterise 95% of the cocoons, while just under 2 were sufficient to describe 50% (Table 5). UPOV and UCL showed similar values of 2.6 and 3.0 for the higher variability threshold, and just over one class was needed to describe 50%. As

TABLE 5 Number of colours or colour groups required to account for 50% and 95% of the observations within each silkworm strain

Reference	50% of observations			95% of observations		
	Min	Max	Average	Min	Max	Average
RHS	1	4	1.7	2	13	6.2
UPOV	1	2	1.1	1	4	2.6
UCL	1	2	1.2	1	6	3.0
CA	1	1	1	1	3	1.4

expected, the classification based on the CA-derived groups proved to be the most concise, with an average of 1.4 classes sufficient to account for 95% of the variability within each strain.

In terms of internal consistency, classification systems are expected to cluster individual measurements into groups with minimal internal variability, such that all observations within a group are perceived by the human eye as the same colour or colour type. In this respect, the RHS classification exhibited the lowest internal variability, with a mean ΔE^* of 1.88 and a maximum value consistently below 5.30. The UPOV system showed the highest mean $\Delta E^* = 4.3$, and also displayed substantial variability, with colour differences within a single category occasionally exceeding 8. The UCL system, with a mean ΔE^* of 3.44, maintained all intra-group differences below a maximum of 5.54, broadly comparable to CA, which recorded a mean ΔE^* of 3.66 and a maximum of 4.8 (data shown in Figure S3 in the Supplementary materials).

These data can be further analysed as shown in Figure 6, where each pairwise difference in the dataset is associated with the 'name switch' frequency, that is, whether the naming system assigns different names or retains the same one at a given ΔE^*, where the greater the distance between two measurements, the higher the likelihood that they will be assigned different colour names.

The full range of variation for RHS is contained between $\Delta E^* = 0$ and 5. In contrast, UCL and CA span a broader range, both approaching saturation at $\Delta E^* = 10$. The steepest part of the UCL curve lies primarily between 0 and 7, whereas CA displays most of its variation above $\Delta E^* \approx 4$. UPOV closely follows UCL up to a ΔE^* of approx. 4, after which it diverges significantly, remaining consistently lower and reaching saturation only at ΔE^* values around 14. This suggests that below this threshold, UPOV tends not to differentiate well between colours, even when all other systems already exhibit a 100% probability of detecting a difference.

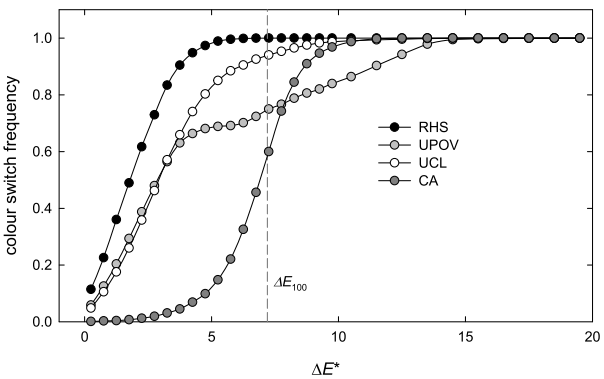

FIGURE 6 Relationship between distances in colorimetric measurements and the probability of assigning different colour names by four classification systems.

For example, at ΔE_{100} RHS detects differences with a probability of 99.9%, UCL at 94.5%, UPOV reaches 74.9%, whereas CA does not exceed 60%, meaning it fails to detect differences in approximately 40% of cases.

4 Discussion

Based on our findings, a thorough description of the cocoon colour variability within a wide-ranging and representative group of silkworm strains can be presented, deriving some useful guidelines about how to implement colorimetric assessment in germplasm characterization for this species.

Measurement geometry and data processing

In colourimetry, similarity between SCI and SCE modes indicates a matte, uniformly textured surface with negligible specular reflection. For silk cocoons, this means the specular component does not affect perceived colour under measurement conditions, ensuring consistent appearance is important for sericulture quality control and textile raw material selection.

The findings from the comparison of CIEDE2000 with alternative formulas utilised in the computation of colour distance corroborate the results reported in

other research that examine this formula in contrast to CIE76 and other formulas utilised in distinct domains of application (Gibert *et al.*, 2005; Gomez-Polo *et al.*, 2016; Hauptmann *et al.*, 2012; Luo *et al.*, 2004).

The perceptibility threshold of 3.65 is consistent with other studies using the CIEDE2000 model across diverse fields. Reported tolerance thresholds generally range from 3-10 ΔE^*, with approx. 3 ΔE^* often representing the upper limit of acceptable perceptibility in food and clinical applications (Fernández-Vázquez *et al.*, 2013; Ghinea *et al.*, 2010), while differences above 5-6 ΔE^* are usually considered substantial and unacceptable when chromatic uniformity is required (Mokrzycki and Tatol, 2011; Silva *et al.*, 2019). Overall, the CIEDE2000 model provides robust quantitative criteria for distinguishing marginally acceptable from clearly significant differences, depending on context.

Overall variability in the $L^*a^*b^*$ colour space: patterns, clustering

The analysis clearly revealed that measurements were concentrated within specific regions of the colour space. In particular, the patterns observed in the a^* and b^* parameters are consistent with the presence of characteristic pigments found in leaves. In the positive range of a^*, carotenoids dominate the coloration, with lutein and β-carotene being the most abundant (Zhu and Zhang, 2014), while Ma and co-authors (Ma *et al.*, 2015) further identified six specific carotenoids in domesticated yellow cocoons, including all-trans-lutein, neoxanthin, violaxanthin, and β-carotene.

The ratio between lutein and β-carotene underlies the formation of different hues: where lutein predominates, cocoons exhibit yellow to golden-yellow tones; conversely, a predominance of β-carotene shifts the colour towards orange-pink shades (Liu *et al.*, 2024). In the present study, for yellow-red colouration, we observed two peaks in a^* and two in b^*, which, when combined, generate four poles defining the vertices of a square in the chromatic space.

For strains producing green cocoons through flavonoid accumulation, variation in green intensity depends both on the total flavonoid content and on the specific types of flavonoid derivatives produced. Mase *et al.* (2023) demonstrated that light-green and deep-green cocoons differ in both the quantity and quality of their flavonoid content. In other words, a higher concentration of flavonoids results in a darker, more intense green, whereas structural differences in the flavonoids can modify the hue. In our data, the green cocoons are those in which the linear variation in the a^*b^* plane is most evident, particularly showing a radial pattern in which hue remains constant, reflecting variation in pigment concentration.

In conclusion, the shape of the colour distribution in $L^*a^*b^*$ space can provide insights into the underlying biochemical complexity: an elongated distribution along a single axis indicates that one pigment (or a co-varying pigment set) drives the chromatic change (e.g. Suzuki *et al.* 2024), whereas a more dispersed distribution points to multiple, independent pigment contributions or more complex chemical interactions. In our measurements, where we observed almost exclusively linear variations, we infer that they are determined by relatively simple chemistry. Accordingly, CIELAB colorimetric measurements can be considered reliable indicators of pigment content.

Cluster analysis

Clustering patterns were evident by visual inspection, yet algorithmic classification was challenging due to contiguous groups connected by diffuse point clouds, especially in the yellow-orange range. In some cases, points from different clusters were closer than those within the same cluster. Using an ε threshold of 3.65, seven clusters were identified, though many observations were discarded as noise. While clustering provides a means of grouping colours, the resulting classes are broad and can mask substantial differences, as also noted by Lu *et al.* (2021). The method may be useful for categorising broad "colour types," but wider validation across more strains is needed for consistent application.

Colour classification and naming

The suitability of a classification system depends on its ability to capture the observed range of perceptual differences (0-7.2 ΔE^*), differentiating colours beyond this threshold while retaining gradation within it. RHS offers high precision, exhausting its variability within 0-5, but requires >60 groups to cover 95% of variability, which is too complex to be of practical use. Optimised clustering fits the interval well with only 7 groups but is dataset-dependent and unsuitable as a standard without broader validation. UPOV is inadequate, failing to distinguish even large differences (>7 ΔE^*) and showing strong imbalance (e.g. "medium light orange" grouping nearly half the strains). UCL extends to 0-10, saturates near 7, uses only 18 groups, and distributes colours more evenly, representing a practical compromise between accuracy and usability. Overall, RHS is most precise, clustering most efficient but non-standardisable, while

UCL emerges as the most balanced and applicable system, especially via commercial colour charts.

Within strain colour difference between years

Environmental variability is expected to play a crucial role in the variability of colours, since it primarily influences leaf characteristics, but it can also impact physiology of insects despite they are reared under controlled conditions, with effects on pigment production. In this study, the only environment-related variability factor which could be controlled, is represented by the years, which has proven to be higher respect to the within-year variability.

The observed interannual variability can plausibly be attributed to changes in the biochemical composition of the leaves. Currently, to our knowledge, no specific data are available for mulberry concerning interannual variations in pigment content; however, such patterns have been more extensively investigated in forest species, where fluctuations in leaf biochemistry are often regarded as adaptive traits in response to climatic variability.

For instance, drier years have been shown to cause a decrease in carotenoid content in two *Quercus* species, (Mészáros *et al.*, 2007), whereas warmer years tend to be associated with higher carotenoid concentrations (Szőllősi *et al.*, 2011). Consistent interannual variation in carotenoids has also been reported for *Nothofagus alpina*, primarily linked to humidity and shading conditions (Arias-Rios *et al.*, 2022).

Similarly, flavonoids are highly responsive to climatic factors: in *Populus tremula*, their concentrations increase during years with enhanced UV-B radiation (e.g. years with lower overall cloud cover), but decline under elevated temperature (Randriamanana *et al.*, 2015). A pronounced interannual variability of phenolic compounds, including flavonoids, has likewise been documented in *Fagus sylvatica*, in association with thermal, water and nutrient stress (Steen *et al.*, 2021)

Whatever the origin of variability, the principal question addressed in this study is whether the observed variability could compromise the stability of colour identification, a factor inherently dependent on the acceptance threshold for colour distance. The present findings indicate that, for the majority of strains, variability remained within acceptable limits when applying the ΔE_{100} threshold across the three-year assessment. Nevertheless, these results should be interpreted with caution, as the stability of this threshold may vary according to strain-specific traits and environmental influences. Broader evaluations, encompassing diverse germplasm and extended temporal and ecological scales, will be required to substantiate the robustness of ΔE_{100} as a reliable criterion for colour identification.

5 Conclusions

Cocoon colour in *Bombyx mori* is a genetically determined yet environmentally modulated trait, with potential as a strain marker. Analysis of 65 naturally coloured strains over three seasons showed that intra-strain variability generally remains within the threshold that was identified as the maximum acceptable (ΔE_{100} = 7.2), though interannual variation may exceed it in some cases. Two chromatic variability patterns – radial and non-radial – were identified on the CIELAB a^*b^* plane. Cluster analysis revealed discrete chromatic classes, with most strains concentrated in yellow and yellow-gold groups. Among classification systems tested, standardised clustering provided the most robust framework, while the combined UCL-RHS approach offered an effective compromise between resolution and practicality. Objective colour measurements should be integrated into silkworm straining and conservation programmes to enhance the characterisation and valorisation of sericultural genetic resources.

Supplementary materials

Data is available on https://doi.org/10.1163/23524588-bja10334 under Supplementary Materials.

Conflict of interest

The authors have no conflict of interest to declare.

Funding statement

The authors were supported by the ARACNE Project, funded by the European Union's Horizon Europe research and innovation programme under the Grant Agreement No 101095188.

References

Afonso, T., Moresco, R., Uarrota, V.G., Navarro, B.B., Nunes, E.d.C., Maraschin, M. and Rocha, M., 2017. UV-Vis and

CIELAB based chemometric characterization of manihot esculenta carotenoid contents. Journal of Integrative Bioinformatics 14: 2017056. https://doi.org/10.1515/jib-2017-0056

Aimjongjun, S., Sutheerawattananonda, M. and Limpeanchob, N., 2013. Silk lutein extract and its combination with vitamin e reduce UVB-mediated oxidative damage to retinal pigment epithelial cells. Journal of Photochemistry and Photobiology B: Biology 124: 34-41. https://doi.org/10.1016/j.jphotobiol.2013.04.003

Arias-Rios, J.A., El Mujtar, V.A., Pastorino, M. and Marchelli, P., 2022. Genetic variation of leaf pigment content in a southern beech. Trees – Structure and Function 36: 1823-1836. https://doi.org/10.1007/s00468-022-02330-z

Ayour, J., Sagar, M., Alfeddy, M.N., Taourirte, M. and Benichou, M., 2016. Evolution of pigments and their relationship with skin color based on ripening in fruits of different Moroccan genotypes of apricots (*Prunus armeniaca* L.). Scientia Horticulturae 207: 168-175. https://doi.org/10.1016/j.scienta.2016.05.027

Biganeh, H., Kabiri, M., Zeynalpourfattahi, Y., Costa Brancalhão, R.M., Karimi, M., Shams Ardekani, M.R. and Rahimi, R., 2022. *Bombyx mori* cocoon as a promising pharmacological agent: A review of ethnopharmacology, chemistry, and biological activities. Heliyon 8: e10496. https://doi.org/10.1016/j.heliyon.2022.e10496

Cao, T.T. and Zhang, Y.Q., 2016. Processing and characterization of silk sericin from *Bombyx mori* and its application in biomaterials and biomedicines. Materials Science and Engineering C 61: 940-952. https://doi.org/10.1016/j.msec.2015.12.082

Chen, J., Ye, H., Wang, J. and Zhang, L., 2023. Relationship between Anthocyanin Composition and Floral Color of Hibiscus syriacus. Horticulturae 9: 48. https://doi.org/10.3390/horticulturae9010048

CIE, 2019. Colorimetry – Part 4: CIE 1976 $L^*a^*b^*$ colour space. Available online at https://cie.co.at/publications/colorimetry-part-4-cie-1976-lab-colour-space-1

Clarke, F.J.J., McDonald, R. and Rigg, B., 1984. Modification to the JPC79 colour-difference formula. Journal of the Society of Dyers and Colourists 100: 128-132. https://doi.org/10.1111/j.1478-4408.1984.tb00969.x

Conesa, A., Manera, F.C., Brotons, J.M., Fernandez-Zapata, J.C., Simón, I., Simón-Grao, S., Alfosea-Simón, M., Martínez Nicolás, J.J., Valverde, J.M. and García-Sanchez, F., 2019. Changes in the content of chlorophylls and carotenoids in the rind of Fino 49 lemons during maturation and their relationship with parameters from the CIELAB color space. Scientia Horticulturae 243: 252-260. https://doi.org/10.1016/j.scienta.2018.08.030

Daimon, T., Hirayama, C., Kanai, M., Ruike, Y., Meng, Y., Kosegawa, E., Nakamura, M., Tsujimoto, G., Katsuma, S. and Shimada, T., 2010. The silkworm Green b locus encodes a quercetin 5-O-glucosyltransferase that produces green cocoons with UV-shielding properties. Proceedings of the National Academy of Sciences of the United States of America 107: 11471-11476. https://doi.org/10.1073/pnas.1000479107

Dong, Z., Xia, Q. and Zhao, P., 2022. Antimicrobial components in the cocoon silk of silkworm, *Bombyx mori*. International Journal of Biological Macromolecules 224: 68-78. https://doi.org/10.1016/j.ijbiomac.2022.10.103

Ester, M., Kriegel, H.-P., Sander, J. and Xu, X., 1996. A density-based algorithm for discovering clusters in large spatial databases with noise. In: Proceedings of the Second International Conference on Knowledge Discovery and Data Mining, 2-4 August 1996, Portland, Oregon, 96, pp. 226-231.

Fernández-Vázquez, R., Stinco, C.M., Hernanz, D., Heredia, F.J. and Vicario, I.M., 2013. Colour training and colour differences thresholds in orange juice. Food Quality and Preference 30: 320-327. https://doi.org/10.1016/j.foodqual.2013.05.018

Ghinea, R., Pérez, M.M., Herrera, L.J., Rivas, M.J., Yebra, A. and Paravina, R.D., 2010. Color difference thresholds in dental ceramics. Journal of Dentistry 38: e57-e64. https://doi.org/10.1016/j.jdent.2010.07.008

Gibert, J.M., Dagà, J.M., Gilabert, E.J., Valldeperas, J. and The Colorimetry Group, 2005. Evaluation of colour difference formulae. Coloration Technology 121: 147-152. https://doi.org/10.1111/j.1478-4408.2005.tb00265.x

Gomez-Polo, M., Portillo, M., Luengo, M., Vicente, P., Galindo, P. and María, M., 2016. A comparison of the CIELab and CIEDE2000 color difference formulas. The Journal of Prosthetic Dentistry 115: 65-70. https://doi.org/10.1016/j.prosdent.2015.07.001

Hauptmann, M., Pleschberger, H., Mai, C., Follrich, J. and Hansmann, C., 2012. The potential of color measurements with the CIEDE2000 equation in wood science. European Journal of Wood and Wood Products 70: 415-420. https://doi.org/10.1007/s00107-011-0575-6

Hirayama, C., Mase, K., Iizuka, T., Takasu, Y., Okada, E. and Yamamoto, K., 2018. Deficiency of a pyrroline-5-carboxylate reductase produces the yellowish green cocoon 'Ryokuken' of the silkworm, *Bombyx mori*. Heredity 120: 422-436. https://doi.org/10.1038/s41437-018-0051-8

Huse, R.D. and Kelly, K.L., 1984. A Contribution Towards standardization of color names in horticulture: application of the universal color language to the colors of the Royal Horticultural Society's Colour Chart. The American Rhododendron Society, Tigard, OR.

Kakihara, N., Sato, M., Shirai, A., Koguchi, M., Yamauchi, S., Nakano, T., Sasamoto, R. and Sato, H., 2024. Green cocoon-derived sericin reduces cellular damage caused by radiation in human keratinocytes. Scientific Reports 14: 3068. https://doi.org/10.1038/s41598-024-53712-x

Kruskal, J.B., 1964. Nonmetric multidimensional scaling: a numerical method. Psychometrika 29: 115-129. https://doi.org/10.1007/BF02289694

Kurioka, A. and Yamazaki, M., 2002. Purification and identification of flavonoids from the yellow green cocoon shell (sasamayu) of the silkworm, *Bombyx mori*. Bioscience, Biotechnology, and Biochemistry 66: 1396-1399. https://doi.org/10.1271/BBB.66.1396

Lancaster, J.E., Lister, C.E., Reay, P.F. and Triggs, C.M., 1997. Influence of pigment composition on skin color in a wide range of fruit and vegetables. Journal of the American Society for Horticultural Science 122: 594-598. https://doi.org/10.21273/JASHS.122.4.594

Liceaga, A.M., 2025. Entomoceuticals: insects as food for health. Journal of Insects as Food and Feed 11: 1859-1865. https://doi.org/10.1163/23524588-20250004

Liu, S., Zhang, Q., Zhou, H., Zhang, B., Yu, M., Wang, Y., Liu, Y. and Chai, C., 2024. The Potential of Natural Carotenoids-Containing Sericin of the Domestic Silkworm *Bombyx mori*. International Journal of Molecular Sciences 25: 3688. https://doi.org/10.3390/ijms25073688

Lu, C., Li, Y., Wang, J., Qu, J., Chen, Y., Chen, X., Huang, H. and Dai, S., 2021. Flower color classification and correlation between color space values with pigments in potted multiflora chrysanthemum. Scientia Horticulturae 283: 110082. https://doi.org/10.1016/j.scienta.2021.110082

Lu, Y., Luo, J., An, E., Lu, B., Wei, Y., Chen, X., Lu, K., Liang, S., Hu, H., Han, M., He, S., Shen, J., Guo, D., Bu, N., Yang, L., Xu, W., Lu, C., Xiang, Z., Tong, X. and Dai, F., 2023. Deciphering the Genetic Basis of Silkworm Cocoon Colors Provides New Insights into Biological Coloration and Phenotypic Diversification. Molecular Biology and Evolution 40: msad017. https://doi.org/10.1093/molbev/msad017

Luo, M., Minchew, C., Kenyon, P. and Cui, G., 2004. Verification of CIEDE2000 using industrial data. In: Proceedings of Interim Meeting of the International Colour Association (AIC 2004 Colour and Paints), 3-5 November 2004, Porto Alegre, Brazil, pp. 97-102.

Luo, M.R., 2002. Development of colour-difference formulae. Review of Progress in Coloration and Related Topics 32: 28-39. https://doi.org/10.1111/j.1478-4408.2002.tb00248.x

Luo, M.R., Cui, G. and Rigg, B., 2001. The development of the CIE 2000 colour-difference formula: CIEDE2000. Color Research and Application 26: 340-350. https://doi.org/10.1002/col.1049

Ma, M., Hussain, M., Dong, S. and Zhou, W., 2015. Characterization of the pigment in naturally yellow-colored domestic silk. Dyes and Pigments 124: 6-11. https://doi.org/10.1016/j.dyepig.2015.08.003

Manupa, W., Wongthanyakram, J., Jeencham, R. and Sutheerawattananonda, M., 2023. Storage stability and antioxidant activities of lutein extracted from yellow silk cocoons (*Bombyx mori*) in Thailand. Heliyon 9: e16805. https://doi.org/10.1016/j.heliyon.2023.e16805

Mase, K., Hirayama, C., Narukawa, J., Kuwazaki, S. and Yamamoto, K., 2023. Fine mapping of Green a, Ga, on chromosome 27 in *Bombyx mori*. Genes and Genetic Systems 98: 239-247. https://doi.org/10.1266/ggs.23-00060

McDonald, R., 1988. Acceptability and Perceptibility decisions using the CMC color difference formula. Textile Chemist and Colorist 20: 31-37.

McDonald, R. and Smith, K.J., 1995. CIE94 – a new colour-difference formula. Journal of the Society of Dyers and Colourists 111: 376-379. https://doi.org/10.1111/j.1478-4408.1995.tb01688.x

Melgosa, M., 2016. CIE94, History, Use, and Performance. In: Luo, M.R. (ed.) Encyclopedia of Color Science and Technology. Springer, New York, NY, pp. 191-195. https://doi.org/10.1007/978-1-4419-8071-7_13

Mészáros, I., Veres, S., Kanalas, P., Oláh, V., Szőllősi, E., Sárvári, É., Lévai, L. and Lakatos, G., 2007. Leaf growth and photosynthetic performance of two co-existing oak species in contrasting growing seasons. Acta Silvatica et Lignaria Hungarica 3: 7-20. https://doi.org/10.37045/aslh-2007-0001

Mokrzycki, W. and Tatol, M., 2011. Colour difference ΔE – a survey. Machine Graphic and Vision 20: 383-411. https://www.researchgate.net/publication/236023905

Moore, S.B. and Ausley, L.W., 2004. Systems thinking and green chemistry in the textile industry: concepts, technologies and benefits. Journal of Cleaner Production 12: 585-601. https://doi.org/10.1016/S0959-6526(03)00058-1

Office of the American Rhododendron Society, 2025. ISCC-NBS Color Names For the Colors Included In the RHS Colour Chart (1966, 1986, 1995, and 2001 Editions). Available online at https://www.arsoffice.org/colorcharts.htm

Omar, A., Wali, A., Arken, A., Gao, Y., Aisa, H.A. and Yili, A., 2022. Covalent binding of flavonoids with silk sericin hydrolysate: Anti-inflammatory, antioxidant, and physicochemical properties of flavonoid-sericin hydrolysate conjugates. Journal of Food Biochemistry 46: e14125. https://doi.org/10.1111/jfbc.14125

Oxman, N., 2015. Templating Design for Biology and Biology for Design. Architectural Design 85: 100-107. https://doi.org/10.1002/ad.1961

Oxman, N., Laucks, J., Kayser, M., Uribe, C.D.G. and Duro-Royo, J., 2013. Biological Computation for Digital Design and Fabrication. In: Proceedings of the Computation and Performance-31st eCAADe Conference, 18-20 September 2013, Delft, The Netherlands, Volume 1, pp. 585-594.

Promphet, P., Bunarsa, S., Sutheerawattananonda, M. and Kunthalert, D., 2014. Immune enhancement activities of silk lutein extract from *Bombyx mori* cocoons. Biological Research 47: 15. https://doi.org/10.1186/0717-6287-47-15

R Core Team, 2022. R: A language and environment for statistical computing (4.2.1). R Foundation for Statistical Computing, Vienna. Available online at https://www.r-project.org/

Randriamanana, T.R., Lavola, A. and Julkunen-Tiitto, R., 2015. Interactive effects of supplemental UV-B and temperature in European aspen seedlings: implications for growth, leaf traits, phenolic defense and associated organisms. Plant Physiology and Biochemistry 93: 84-93. https://doi.org/10.1016/j.plaphy.2015.03.001

Ripley, B., Venables, B., Bates, D.M., Hornik, K., Gebhardt, A. and Firth, D., 2023. MASS: Support Functions and Datasets for Venables and Ripley's MASS. Available at: https://CRAN.r-project.org/package=MASS

Robertson, A.R., 1977. The CIE 1976 Color-Difference Formulae. Color Research and Application 2: 7-11. https://doi.org/10.1002/j.1520-6378.1977.tb00104.x

Robinson, T., McMullan, G., Marchant, R. and Nigam, P., 2001. Remediation of dyes in textile effluent: a critical review on current treatment technologies with a proposed alternative. Bioresource Technology 77: 247-255. https://doi.org/10.1016/S0960-8524(00)00080-8

Royal Horticultural Society, 1966. Colour Chart. 1st ed. Royal Horticultural Society, Kew.

Sánchez Beeckman, M., 2022. ColorNameR: Give Colors a Name. R package version 0.1.0 (0.1.0). Available online at https://cran.r-project.org/web/packages/ColorNameR/index.html

Sharma, G., Wu, W. and Dalal, E.N., 2005. The CIEDE2000 color-difference formula: Implementation notes, supplementary test data, and mathematical observations. Color Research and Application 30: 21-30. https://doi.org/10.1002/col.20070

Silva, C.E.d.F., Abud, A.K.d.S., da Silva, I.C.C., Andrade, N.P., Cerqueira, R.B.d.O., de Andrade, F.P., Carvalho, F.d.O., Almeida, R.M.R.G. and de Souza, J.E.A., 2019. Acceptability of tropical fruit pulps enriched with vegetal/microbial protein sources: viscosity, importance of nutritional information and changes on sensory analysis for different age groups. Journal of Food Science and Technology 56: 3810-3822. https://doi.org/10.1007/s13197-019-03852-0

Singha, S., Baugher, T.A., Townsend, E.C. and D'Souza, M.C., 1991. Anthocyanin distribution in 'delicious' apples and the relationship between anthocyanin concentration and chromaticity values. Journal of the American Society for Horticultural Science 116: 497-499. https://doi.org/10.21273/JASHS.116.3.497

Singhrang, N., Tocharus, C., Thummayot, S., Sutheerawattananonda, M. and Tocharus, J., 2018. Protective effects of silk lutein extract from *Bombyx mori* cocoons on β-Amyloid peptide-induced apoptosis in PC12 cells. Biomedicine and Pharmacotherapy 103: 582-587. https://doi.org/10.1016/j.biopha.2018.04.045

Steen, J.S., Asplund, J., Lie, M.H. and Nybakken, L., 2021. Environment rather than provenance explains levels of foliar phenolics in European beech (*Fagus sylvatica* L.) seedlings. Trees Structure and Function 35: 1555-1569. https://doi.org/10.1007/s00468-021-02136-5

Suzuki, T., Ito, C., Kitano, K. and Yamaguchi, T., 2024. CIELAB color space as a field for tracking color-changing chemical reactions of polymeric pH indicators. ACS Omega 9: 36682-36689. https://doi.org/10.1021/acsomega.4c05320

Szőllősi, E., Oláh, V., Kanalas, P., Kis, J., Nyitrai, B., Sárvári, É., Solti, Á. and Mészáros, I., 2011. Physiological responses of two co-existing oak species in years with contrasting climatic conditions. Acta Biologica Szegediensis 55: 169-174. https://abs.bibl.u-szeged.hu/index.php/abs/article/view/2742

Tabunoki, H., Higurashi, S., Ninagi, O., Fujii, H., Banno, Y., Nozaki, M., Kitajima, M., Miura, N., Atsumi, S., Tsuchida, K., Maekawa, H. and Sato, R., 2004. A carotenoid-binding protein (CBP) plays a crucial role in cocoon pigmentation of silkworm (*Bombyx mori*) larvae. FEBS Letters 567: 175-178. https://doi.org/10.1016/j.febslet.2004.04.067

Takechi, T., Maekawa, Z.-I. and Sugimura, Y., 2011. Food Science and Technology Research 17: 493-497. https://doi.org/10.3136/fstr.17.493

Tanaka, Y., 1913. A study of Mendelian factors in the silkworm, *Bombyx mori*. The Journal of the College of Agriculture, Tohoku Imperial University, Sapporo, Japan 5: 91-113. http://hdl.handle.net/2115/12514

Tian, Z., Zhao, C., Huang, T., Yu, L., Sun, Y., Tao, Y., Cao, Y., Du, R., Lin, W. and Zeng, J., 2024. Silkworm cocoon: dual functions as a traditional chinese medicine and the raw material of promising biocompatible carriers. Pharmaceuticals 17: 817. https://doi.org/10.3390/ph17070817

Tocharus, C. and Sutheerawattananonda, M., 2024. Hypoglycemic Ability of Sericin-Derived Oligopeptides (SDOs) from *Bombyx mori* Yellow Silk Cocoons and Their Physiological Effects on Streptozotocin (STZ)-Induced Diabetic Rats. Foods 13: 2184. https://doi.org/10.3390/foods13142184

Tsuchida, K. and Sakudoh, T., 2015. Recent progress in molecular genetic studies on the carotenoid transport system using cocoon-color mutants of the silkworm. Archives of Biochemistry and Biophysics 572: 151-157. https://doi.org/10.1016/j.abb.2014.12.029

Venables, W.N. and Ripley, B.D., 2002. Modern applied statistics with S. 4th ed. Springer, New York, NY.

Voss, D.H., 2002. The Royal Horticultural Society colour chart 2001. Journal of the American Rhododendron Society 56: 10-11. Available online at https://scholar.lib.vt.edu/ejournals/JARS/v56n1/v56n1-voss.html

Voss, D.H. and Hale, W.N., 1998. A comparison of the three editions of the Royal Horticultural Society colour chart. HortScience 33: 13-17. https://eurekamag.com/research/003/019/003019660.php

Wang, H.Y., Wang, Y.J., Zhou, L.X., Zhu, L. and Zhang, Y.Q., 2012. Isolation and bioactivities of a non-sericin component from cocoon shell silk sericin of the silkworm *Bombyx mori*. Food and Function 3: 150-158. https://doi.org/10.1039/c1fo10148j

Wang, H.Y., Zhao, J.G. and Zhang, Y.Q., 2020. The flavonoid-rich ethanolic extract from the green cocoon shell of silkworm has excellent antioxidation, glucosidase inhibition, and cell protective effects *in vitro*. Food and Nutrition Research 64: 1-12. https://doi.org/10.29219/fnr.v64.1637

Wang, Y., Gao, J., Yang, Y., Zhu, L., Yang, W., Li, P., Yang, W. and Yang, W., 2025. A Review on the Extraction Methods, Bioactivities, and Application in Foods of Silk Sericin. Journal of Food Biochemistry: 2155701. https://doi.org/10.1155/jfbc/2155701

Zhao, J.G., Wang, H.Y., Wei, Z.G. and Zhang, Y.Q., 2019. Therapeutic effects of ethanolic extract from the green cocoon shell of silkworm *Bombyx mori* on type 2 diabetic mice and its hypoglycaemic mechanism. Toxicology Research 8: 407-420. https://doi.org/10.1039/c8tx00294k

Zhu, L. and Zhang, Y.-Q., 2014. Identification and analysis of the pigment composition and sources in the colored cocoon of the silkworm, *Bombyx mori*, by HPLC-DAD. Journal of Insect Science 14: 31. https://doi.org/10.1093/jis/14.1.31